Supramolecular Chemistry
Publication details, including instructions for authors and subscription information:
http://www.informaworld.com/smpp/title~content=t713649759

Guest-induced conformation shift of *p*-sulphonatothiacalix[4]arene in the solid state and solution manipulated by $[Zn(dipy)_3]^{2+}$

Asiya Mustafina[a]; Margit Gruner[a]; Aidar Gubaidullin[a]; Sergey Katsyuba[a]; Viktoriya Skripacheva[a]; Elena Zvereva[a]; Sofiya Kleshnina[a]; Wolf-Dieter Habicher[a]; Svetlana Soloveva[a]; Alexander Konovalov[a]
[a] A.E. Arbuzov Institute of Organic and Physical Chemistry, Kazan, Russia

First published on: 17 February 2010

To cite this Article Mustafina, Asiya , Gruner, Margit , Gubaidullin, Aidar , Katsyuba, Sergey , Skripacheva, Viktoriya , Zvereva, Elena , Kleshnina, Sofiya , Habicher, Wolf-Dieter , Soloveva, Svetlana and Konovalov, Alexander(2010) 'Guest-induced conformation shift of *p*-sulphonatothiacalix[4]arene in the solid state and solution manipulated by $[Zn(dipy)_3]^{2+}$', Supramolecular Chemistry, 22: 4, 203 — 211, First published on: 17 February 2010 (iFirst)
To link to this Article: DOI: 10.1080/10610270903254159
URL: http://dx.doi.org/10.1080/10610270903254159

Supramolecular Chemistry
Vol. 22, No. 4, April 2010, 203–211

Taylor & Francis
Taylor & Francis Group

Guest-induced conformation shift of *p*-sulphonatothiacalix[4]arene in the solid state and solution manipulated by $[Zn(dipy)_3]^{2+}$

Asiya Mustafina*, Margit Gruner, Aidar Gubaidullin, Sergey Katsyuba, Viktoriya Skripacheva, Elena Zvereva, Sofiya Kleshnina, Wolf-Dieter Habicher, Svetlana Soloveva and Alexander Konovalov

A.E. Arbuzov Institute of Organic and Physical Chemistry, Arbuzov Street, 8, 420088 Kazan, Russia

(*Received 6 May 2009; final version received 29 July 2009*)

The ^{1}H NMR and X-ray analysis data reveal the guest-induced *cone* → *partial cone* and *cone* → *1,2-alternate* conformational shift in aqueous methanol solutions and solid state for a *p*-sulphonatothiacalix[4]arene-$[Zn(dipy)_3]^{2+}$ host–guest system. The experimental data, together with DFT calculations, show that the guest-induced conformational shift of *p*-sulphonatothiacalix[4]arene is facilitated by the deprotonation of phenolic groups.

Keywords: *p*-sulphonatothiacalix[4]arene; *partial cone*; *1,2-alternate*; inclusion complex

Introduction

Sulphonated calix[*n*]arenes and their thia-analogues have gained much attention as promising building blocks in supramolecular chemistry during recent decades (*1–9*). Such enhanced interest is underlain by the great diversity of the wonderful supramolecular structures of their inclusion and metal complexes (*2–9*). This diversity in turn has resulted from the multi-functional complexation ability of sulphonated calix[*n*]arenes and a variety of their conformational states. Thiacalix[4]arene tetrasulphonate (TCAS) is of particular interest as the host molecule and building block of supramolecular structures due to its unique inclusion and binding abilities towards metal complexes, organic molecules and metal ions (*5–9*). It is also worth noting that TCAS is more conformationally flexible than its classical counterpart *p*-sulphonatocalix[4]arene (CAS) (*9*), which facilitates a guest-induced conformational shift, resulting in the additional diversity of supramolecular structures. Although, in the majority of TCAS-based inclusion complexes, the host molecules adopt a *cone* conformation (*5*, *6*), there are some interesting examples of the guest-manipulated conformational shift from *cone* to *partial cone* and *1,2-alternate* (*7*, *8*). The analysis of the literature data reveals two main factors manipulating the diversity of TCAS conformations in host–guest complexes: (i) the shape and the size of the guest (*7*) and (ii) the pH of solutions used to obtain the complexes (*8*). It is well known that the *cone* conformations of TCAS, as well as CAS, are stabilised by the intramolecular hydrogen bonding (*10*, *11*). Thus, the energy losses caused by the distortion of the *cone* conformation should be compensated by host–guest interactions. From this standpoint, the pH value of a solution where the host–guest binding occurs is of particular importance, since the deprotonation of the phenolic rim caused by the pH increase weakens the circular hydrogen bonding on the lower rim. Thus, the pH increase should be regarded as a crucial factor, providing both kinetic and thermodynamic favouring of the conformational conversion.

The guest size effect can be revealed within the series of tris-dipyridyls of transition metals with the varied length of a metal–ligand bond. In particular, the metal–nitrogen bond length grows in the series $[Co(dipy)_3]^{3+} > [Ru(dipy)_3]^{2+} > [Zn(dipy)_3]^{2+}$ (*12–14*). According to our previous X-ray and ^{1}H NMR data, tris-dipyridyls of Co(III) and Ru(II) are included into the TCAS adopting a *pinched cone* conformation, which enhances the CH-π host–guest interactions (*15*). The present work shows the guest ($[Zn(dipy)_3]^{2+}$)-induced *cone* → *partial cone* and *cone* → *1,2-alternate* shift of the TCAS conformation in the solid state and aqueous methanol solutions. The X-ray analysis and ^{1}H NMR spectral data, as well as the DFT computations of *p*-sulphonatothiacalix[4]arene ($TCAS^{4-}$) and its deprotonated species ($TCAS^{5-}$, $TCAS^{6-}$ and $TCAS^{8-}$), are introduced to reveal the effect of pH on the guest-induced conformational shift of TCAS.

Experimental section

TCAS and $[Zn(dipy)_3](ClO_4)_2$ were synthesised according to known procedures (*16*, *17*).

The crystalline complex ($[Zn(dipy)_3]^{2+}$)3($TCAS^{6-}$) (**1**) was obtained by slow evaporation of aqueous methanol (50 vol.%) solution of $[Zn(dipy)_3]^{2+}$ and TCAS in a 4:1

*Corresponding author. Email: asiya@iopc.knc.ru

ISSN 1061-0278 print/ISSN 1029-0478 online

DOI: 10.1080/10610270903254159
http://www.informaworld.com

(Zn:TCAS) molar ratio at pH 10. The pH 10 was adjusted by the addition of the required amounts of sodium alkaline solution.

NMR measurements

The NMR experiments were performed on a Bruker DRX-500 spectrometer operating at 500.13 MHz (^{1}H) and 125.77 MHz (^{13}C). Pulsed z-gradients were used for the COSY, HSQC, HMBC and NOESY measurements. The ^{1}H NMR spectra were recorded in mixed D_2O–CD_3OD solutions using TMS as a standard. The two-dimensional (2D) experiments were acquired with proton spectral widths of 4000 Hz in both dimensions and 2K data points in the t2 domain. Furthermore, the following parameters were used: (a) the COSY spectra were recorded using 512 t1 increments with eight scans; (b) the ^{1}H/^{13}C correlated spectra were recorded with 350 t1 increments, 8 or 32, respectively, transients for each t1, and a long-range delay, $\Delta = 65$ ms, for HMBC; π/3-shifted sine-squared functions for HSQC and, respectively, sine-bell functions for HMBC and a zero-filled 2K × 1K data matrix were used for processing; (c) the phase-sensitive NOESY and ROESY spectra were obtained in the TPPI mode from 512 experiments in t1, 32 scans in t2 and D1 = 2.0 s; mixing time τ_m(NOE) = 800 ms, spinlock-τ_m(ROE) = 250 ms. The data were zero-filled to 2K × 2K points before applying a π/2-shifted sine-squared-bell function in both dimensions. All NMR measurements have been performed in the mixed solvent D_2O–methanol-d^4 with 40 vol.% of the latter at pH 11, which was maintained by the use of Tris (0.01 M).

X-ray analysis

The X-ray diffraction data for the crystal of compound **1** were collected at 296 K on a Bruker AXS Smart Apex II CCD diffractometer in the ω- and φ-scan modes using graphite monochromated Mo K_α ($\lambda = 0.71073$ Å) radiation. The data were corrected for the absorption effect using the SADABS program (*18*). The structures were solved by a direct method and refined by the full-matrix least squares using SHELXTL (*19*) and WinGX (*20*) programs. All non-hydrogen atoms were refined anisotropically. One of the SO_3 groups was disordered over two positions with relative occupancies of 0.45:0.55. The positions of hydrogen atoms were located from the Fourier electron density synthesis and were included in the refinement in the isotropic riding model approximation. Data collections: images were indexed, integrated and scaled using the APEX2 (*21*) data reduction package. All figures were made using PLATON (*22*).

Crystallographic data (excluding structure factors) for structure **1** in this paper have been deposited at the Cambridge Crystallographic Data Centre as supplementary publication number CCDC 728615. Copies of the data can be obtained, free of charge, on application to CCDC, 12 Union Road, Cambridge CB2 1EZ, UK (Fax: +44-(0)1223-336033 or e-mail: deposit@ccdc.cam.ac.uk).

Crystallographic data for ***1***

Formula $C_{24}H_{10}O_{16}S_8$, 3($C_{30}H_{24}N_6Zn$), 10.5(H_2O), pink prism of dimensions $0.33 \times 0.26 \times 0.08$ mm^3, formula weight 2610.74 g mol^{-1}, triclinic, $a = 13.950$ (2), $b = 20.491$ (3), $c = 24.102$ (4) Å, $\alpha = 65.513$ (2)°, $\beta = 76.010$ (2)°, $\gamma = 85.287$ (2)°, $V = 6082.5$ (18) Å^3, $T = 296$ K, space group *P*-1 (No. 2), Z = 2, μ(Mo K_α) = 8.04 cm^{-1}, $F(000) = 2696$, $d_{calc} = 1.425$ g cm^{-3}, 64,549 reflections measured, 25,589 unique ($R_{int} = 0.1432$), restraints/parameters = 117/1533. Final indices $R_1(F) = 0.0697$, $wR_2(F^2) = 0.1217$ using 7749 reflections, with $I > 2\sigma I$, and $R_1(F) = 0.2672$, $wR_2(F^2) = 0.1861$ using all reflections. Goodness-of-fit on F^2 was 0.915. Completeness of data at Theta (max) 27.00° is 0.963.

Computations

All DFT calculations were done using the Gaussian-03 suite of programs (*23*). We used Becke's three-parameter exchange functional (*24*) in combination with the Lee–Yang–Parr correlation functional (B3LYP) (*25*) and the standard 6-31G* basis set. All stationary points were characterised as minima by the analysis of the Hessian matrices.

Results and discussion

The slow evaporation of aqueous methanol solutions at pH 10 of $[Zn(dipy)_3](ClO_4)_2$ (4×10^{-3} M) and TCAS (1×10^{-3} M) results in the growth of single crystal **1** suitable for the X-ray diffraction analysis. The assymetric part of the triclinic unit cell of complex **1** possesses one $TCAS^{6-}$ anion, three $[Zn(dipy)_3]^{2+}$ counterions and 10.5 water molecules. The X-ray analysis reveals that $TCAS^{6-}$ adopts a *partial cone* conformation in **1** (Figure 1), which is very similar to the complex of $TCAS^{4-}$ with $[Ni(dipy)_3]^{2+}$ presented in (*7*). It is worth noting that the inclusion complex of $[Ni(dipy)_3]^{2+}$ with TCAS was synthesised under hydrothermal conditions at pH 1, while the complex with $[Zn(dipy)_3]^{2+}$ was obtained at ambient temperature and pH 10. Figure 2 shows that two $[Zn(dipy)_3]^{2+}$ complexes are interacting with $TCAS^{6-}$ in the inclusion mode. The dipyridyl fragments of the two $[Zn(dipy)_3]^{2+}$ complexes fill two pseudo-cavities of TCAS from both sides. Both $[Zn(dipy)_3]^{2+}$ ions interact with TCAS through C–H···O interactions. The π–π inter-

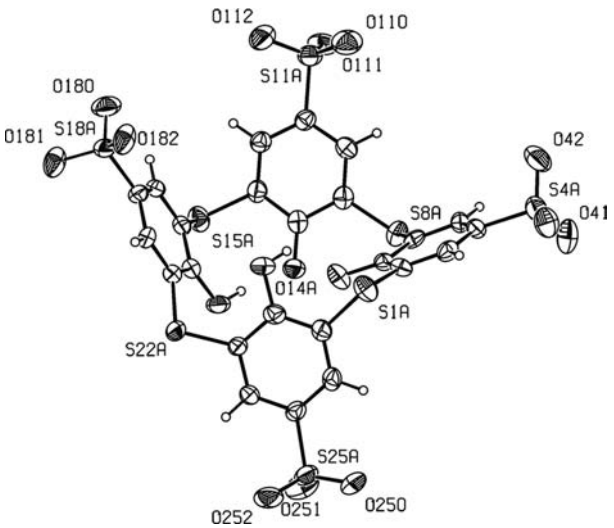

Figure 1. ORTEP drawing of the $TCAS^{6-}$ anion. Displacement ellipsoids are drawn at the 30% probability level. H atoms are represented by circles of arbitrary size.

actions have been revealed only for one of them, which is located within three aromatic rings of TCAS. No direct contacts between calixarene units are revealed, because each calixarene unit is surrounded by 12 $[Zn(dipy)_3]^{2+}$ ions and water molecules. The lack of direct contacts between $[Zn(dipy)_3]^{2+}$ ions has been found, while the numerous hydrogen bondings through water molecules are revealed.

The aqueous methanol alkaline conditions (pH 11) were chosen for the ^1H NMR spectral measurements to evaluate host–guest interactions in the $[Zn(dipy)_3]^{2+}$–TCAS system. The use of neutral (pH 6–8) conditions results in the NMR spectra with rather widened peaks, which hampers their interpretation. The broadening of signals becomes insignificant in alkaline aqueous methanol solutions, thus the ^1H NMR spectra of $[Zn(dipy)_3]^{2+}$ with TCAS, presented in Figure 3, possess some sets of signals, which can be distinguished and analysed. The ^1H NMR spectrum of aqueous methanol solution of $[Zn(dipy)_3]^{2+}$–TCAS at a 1:1 concentration ratio is quite different from the simple overlapping of the spectra of $[Zn(dipy)_3]^{2+}$ and TCAS recorded separately (Figure 3(a)). The ^1H NMR spectrum of $[Zn(dipy)_3]^{2+}$ in aqueous methanol solutions possesses broadened signals of aromatic protons (their chemical shifts are presented in Table 1). The widening of signals results from the dissociation of $[Zn(dipy)_3]^{2+}$ due to its kinetic lability. The ^1H NMR spectrum of TCAS at the same conditions looks similar to a singlet at 8.04 ppm, which is typical for the *cone* conformation. Several NMR procedures, namely NOESY and DOSY (Figures 4 and 5), as well as

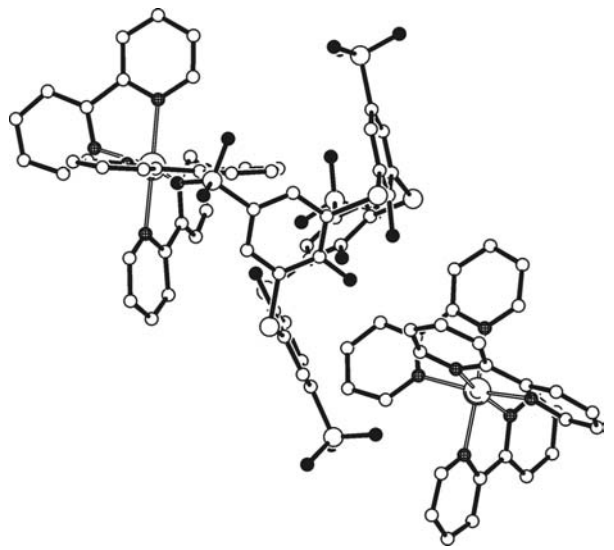

Figure 2. Mutual arrangements of two $[Zn(dipy)_3]^{2+}$ complexes and the $TCAS^{6-}$ anion in the crystal. H atoms are omitted for clarity.

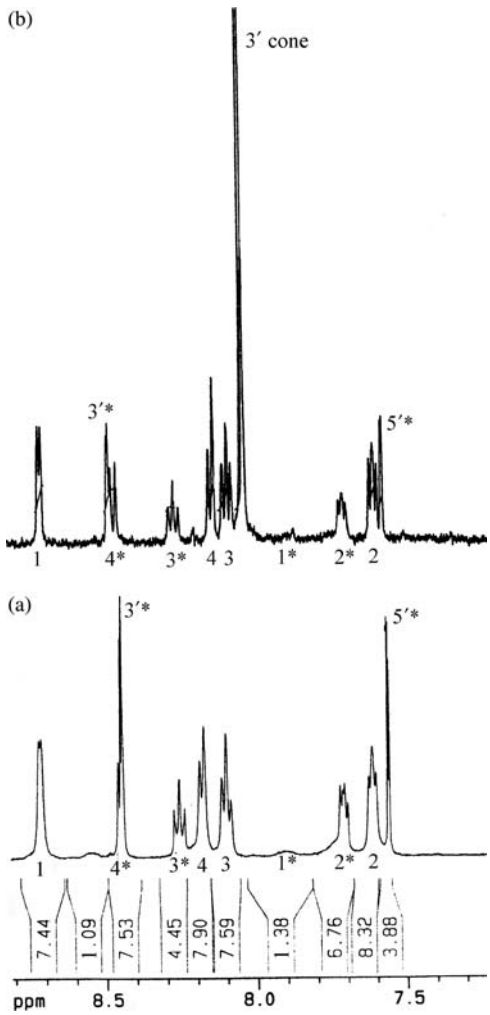

Figure 3. The spectra of aqueous methanol solutions of $[Zn(dipy)_3]^{2+}$ and TCAS at pH 11 (Tris buffer), $C_{Zn} = 0.002$ M at a 1:1 concentration ratio (a) and at the 15-fold excess of TCAS (b). The assignment of protons is shown in Scheme 1.

Table 1. The δ (^{1}H) values of $[Zn(dipy)_3]^{2+}$ in aqueous methanol solution and at a 1:1 (1:2) ($[Zn(dipy)_3]^{2+}$:TCAS) ratio.

Number	4*	3*	2*	1*
Free	8.41	8.10	7.42	7.83
δ(1:1)	8.49	8.25	7.73	7.78
δ(1:2)	8.43	8.27	7.73	7.76
$\Delta\delta$	0.02–0.08	0.15–0.17	0.29	−(0.05–0.07)

COSY, HSQC and HMBC (see Figures S1–S3 in the Supporting Information), have been performed for the accurate assignment of the signals observed.

The most striking difference of the spectra presented in Figure 3(a) from that of TCAS in aqueous methanol solutions is that two signals at 8.44 and 7.55 ppm (marked as 3′* and 5′* in Figure 3(a)) instead of the singlet at 8.04 ppm are observed, which are assigned to TCAS in the *1,2-alternate* conformation. The admixture of the excess amount of TCAS results in the appearance and increasing of the singlet at 8.04 ppm (3′), which is typical for the *cone* in addition to *1,2-alternate* conformations without sufficient changes of the other signals (Figure 3(b)). It is worth noting that aromatic protons of 2,2′-dipyridyl provide two sets of signals: one is 1–4 and another is 1*–4* (Figure 3(a),(b)). The comparison with the spectral pattern of free 2,2′-dipyridyl and $[Zn(dipy)_3]^{2+}$ in aqueous methanol solution shows that signals 1–4 and 1*–4* can be assigned to 2,2′-dipyridyl as a free molecule and bound with Zn(II), respectively. Taking into account that $[Zn(dipy)_3]^{2+}$ is kinetically labile, two sets of signals of dipy protons result from the dissociation of kinetically labile $[Zn(dipy)_3]^{2+}$ according to equilibriums (1) and (2),

$$[Zn(dipy)_3]^{2+} \leftrightarrow [Zn(dipy)_2]^{2+} + dipy, \quad (1)$$

$$[Zn(dipy)_2]^{2+} \leftrightarrow [Zn(dipy)]^{2+} + dipy. \quad (2)$$

The NOESY spectrum reveals the weak intermolecular nuclear Overhauser effects (NOEs) between the host (3′*) and the guest (2* and 3*) and no NOEs between 3′ or 3′* and 1–4 protons (Figure 4). This means that *1,2-alternate*-TCAS is bound with Zn(II) complexes (protons 1*–4*), while dipy molecules resulting from the dissociation of the Zn(II) complex according to equilibriums (1) and (2) are 'free'. The spectrum of 2,2′-dipyridyl (dipy) with TCAS in aqueous methanol solution at a 1:1 concentration ratio looks similar to the simple overlapping of the spectra of TCAS and dipy recorded separately, which confirms the lack of interaction between them. Moreover, the DOSY data show that two kinds of 2,2′-dipyridyl (1–4 and 1*–4*) molecules have quite different diffusion coefficients (Figure 5). In particular, the diffusion coefficients of $[Zn(dipy)_3]^{2+}$ or its dechelated forms ($[Zn(dipy)_2]^{2+}$ and $[Zn(dipy)]^{2+}$) (protons 1*–4*) are very similar to those of *1,2-alternate*-TCAS (protons 3′* and 5′*), but detectably

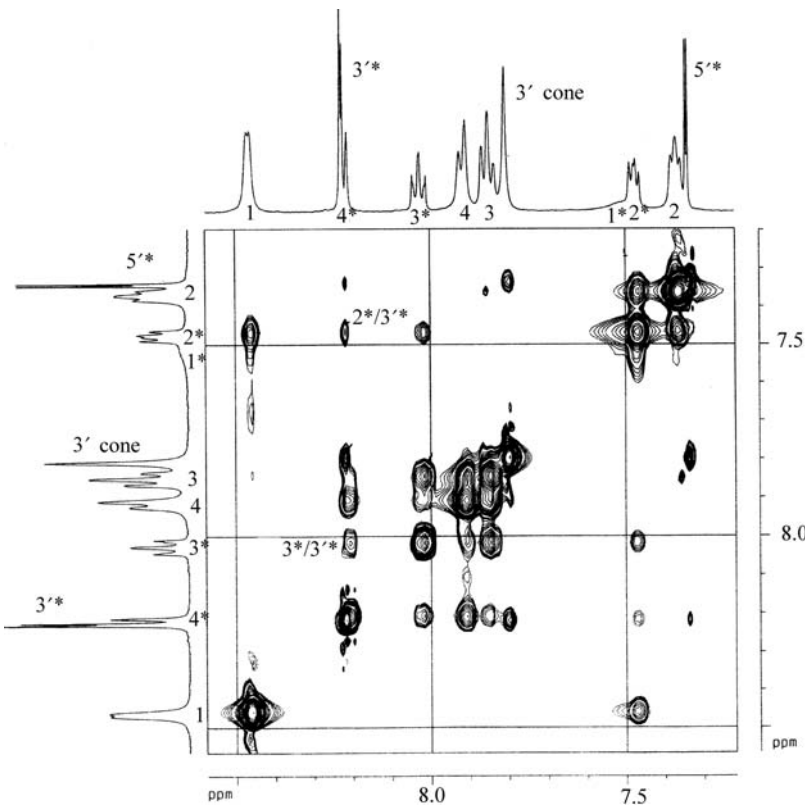

Figure 4. NOESY spectrum of $[Zn(dipy)_3]^{2+}$ and TCAS ($C_{Zn} = 0.002$ M, Zn:TCAS = 1:1) in aqueous methanol solution at pH 11.

lower than those of 'free' 2,2′-dipyridyl molecules (protons 1–4) (see Figure 5). Thus, *1,2-alternate*-TCAS is bound with the dechelated forms ($[Zn(dipy)_n]^{2+}$, $n = 1$, 2), because the analysis of the integrals of proton signals shows some excess of 'free' 2,2′-dipyridyl molecules (1–4) versus the complexed ones (1*–4*).

The chemical shifts of 1*–4* signals at a 1:1 and 1:2 $[Zn(dipy)_3]^{2+}$:TCAS concentration ratio are downfield-shifted versus chemical shifts of $[Zn(dipy)_3]^{2+}$ in aqueous methanol solutions (Table 1). The downfield shift of 3* and 2* proton signals (Table 1) indicates no inclusion-type binding between Zn(II) complex and TCAS (Scheme 1). Taking into account that $[Zn(dipy)_2]^{2+}$ and $[Zn(dipy)]^{2+}$ are not coordinatively saturated, the inner sphere coordination through phenolate groups of *1,2-alternate*-$TCAS^{8-}$ is the most probable binding mode. Since *1,2-alternate*-$TCAS^{8-}$ possesses two symmetric bi- or tridentate coordination sites for Zn(II), it is quite probable that one $TCAS^{8-}$ molecule binds two $[Zn(dipy)_2]^{2+}$ or $[Zn(dipy)]^{2+}$ complexes (Scheme 2). The X-ray structure obtained in alkaline TCAS solutions with copper (II) and imidazole (*8*) confirms the possibility of the structure presented in Scheme 2.

The exchange conditions can be evaluated from the obtained data. The rate constants (k) and activation energy values ($\Delta G^{\#}$) for the exchange processes were evaluated from 2D-EXSY data. The exchange between *cone*-TCAS and *1,2-alternate*-TCAS is characterised by $k = 2.5\,s^{-1}$ and $\Delta G^{\#} = 17.6\,kcal\,mol^{-1}$. The exchange parameters between 2,2′-dipyridyl molecules and those bound with *1,2-alternate*-TCAS are $k = 0.5\,s^{-1}$ and $\Delta G^{\#} = 16.9$ $kcal\,mol^{-1}$.

It is worth noting that these exchange conditions and the mode of $[Zn(dipy)_3]^{2+}$ binding with TCAS are quite different from those of $[Co(dipy)_3]^{3+}$ and $[Ru(dipy)_3]^{2+}$ (*15*). The latter are included into the cavity of TCAS in the outer sphere mode without disrupting its *cone* conformation, which results in the upfield shifting of dipy proton signals (*15*). Both X-ray data in the solid state and ^1H NMR data in solutions in the case of Ru(II) and Co(III) complexes indicate their similar inclusion mode into *cone*-TCAS. To recognise the peculiarity of $[Zn(dipy)_3]^{2+}$, two points are worth discussing. The first point concerns the reason for the different binding modes for $[Zn(dipy)_3]^{2+}$, $[Co(dipy)_3]^{3+}$ and $[Ru(dipy)_3]^{2+}$. Most probably, the inclusion of bulky $[Zn(dipy)_3]^{2+}$ into the cone-shaped cavity of TCAS would not provide the efficient CH–π interaction as in the case of more compact $[Ru(dipy)_3]^{2+}$ and $[Co(dipy)_3]^{3+}$ [for comparison: the Zn—N bond (2.14 Å) is longer than Ru—N (2.06 Å) and Co—N (1.94 Å) bonds (*12–14*)]. This assumption is in good agreement with the weak host–guest interaction between $[Zn(dipy)_3]^{2+}$ and TCAS in neutral aqueous solutions. According to the X-ray data, the *partial cone* conformation of $TCAS^{6-}$ facilitates its interaction with $[Zn(dipy)_3]^{2+}$, while the *cone* → *partial cone* transfer is probably facilitated by alkaline conditions. Although the recent published data (*26*) reveal that CAS adopts the *cone* conformation in the inclusion complex with [Zn(1,10-phenantroline)$(H_2O)_4]^{2+}$, it is not contrary to our data,

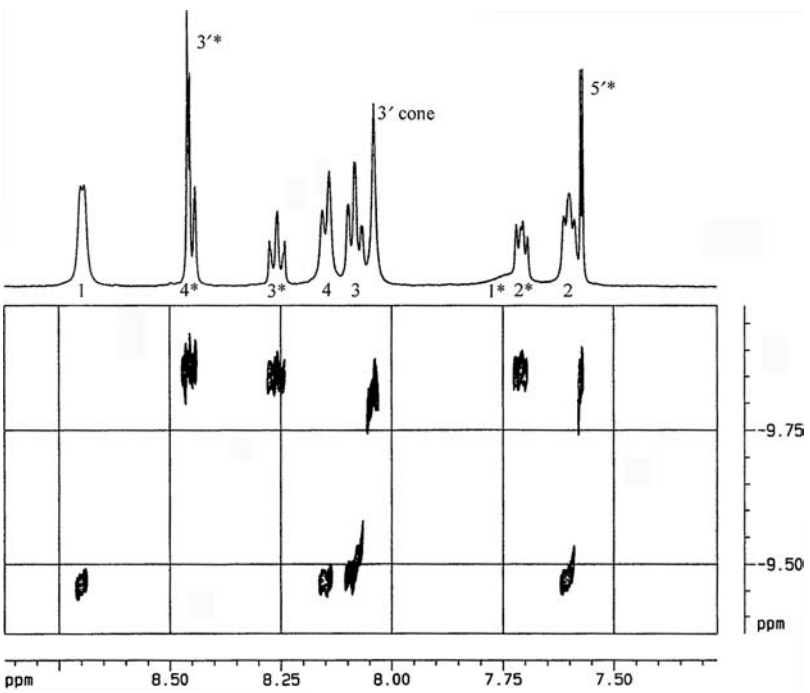

Figure 5. DOSY spectrum of $[Zn(dipy)_3]^{2+}$ and TCAS ($C_{Zn} = 0.002$ M, Zn:TCAS = 1:15) in aqueous methanol solution at pH 11.

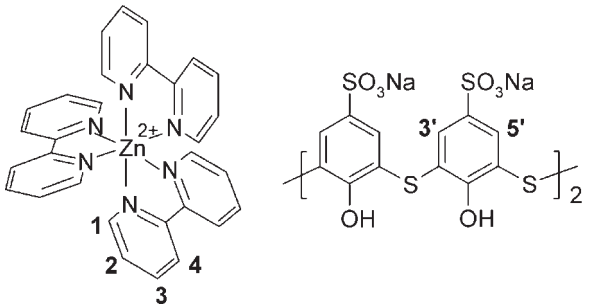

Scheme 1. Designation of TCAS and $[Zn(dipy)_3]^{2+}$ protons.

because the Zn(II) complex with one chelated ligand is much less bulky than that possessing three diimine chelate rings. The NMR data discussed above demonstrate that the guest-induced conformational shift of the host is not necessarily gained from the crystal packing, which suggests a rather high conformational flexibility of TCAS molecules in solutions.

Since the solution conformation of TCAS is different from *partial cone* found by X-ray analysis, the second point worth discussing is the reason for such difference. First of all, the conditions of the NMR measurements and the crystal growth are rather similar but not equal. Unfortunately, only amorphous precipitates can be obtained at the pH conditions, where TCAS is predominantly in the *1,2-alternate* conformation, while the crystals grow at less alkaline conditions, resulting in the broadening of the NMR spectra as mentioned above. Most probably, the X-ray structure, where $TCAS^{6-}$ adopts the *partial cone* conformation and interacts with two $[Zn(dipy)_3]^{2+}$, can be regarded as the intermediate step of the complex formation between *1,2-alternate*-$TCAS^{8-}$ and the dechelated forms of the Zn(II) complex. This in turn raises an issue about the easiness of the *partial cone* → *1,2-alternate* conformational transformation. To shed light on the conformational behaviour of the

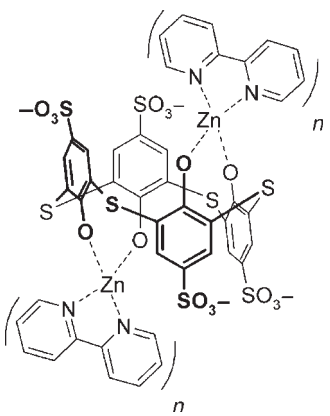

Scheme 2. Schematic representation of the binding mode between *1,2-alternate*-$TCAS^{8-}$ and $[Zn(dipy)_n]^{2+}$ ($n = 1, 2$).

Table 2. Optimised conformations of $TCAS^{4-}$ and their conformational energies (ΔE) relative to the electronic energies (E) of the most stable conformer.

Conformations	E (a.e.u.)	ΔE (kcal mol^{-1})
Cone-C4	− 5310.6289	0
Paco	− 5310.6164	7.9
1,2-alt	− 5310.6141	9.3
1,3-alt	− 5310.6046	15.3
Cone-C2	− 5310.5917	23.4

title compound as dictated by various pH of the solvent, we performed DFT computations of *p*-sulphonatothiacalix[4]-arene ($TCAS^{4-}$) and its deprotonated species ($TCAS^{5-}$, $TCAS^{6-}$ and $TCAS^{8-}$).

As it would be expected, all four stable conformations typical for calix[4]arenes and thiacalix[4]arenes (*cone*,

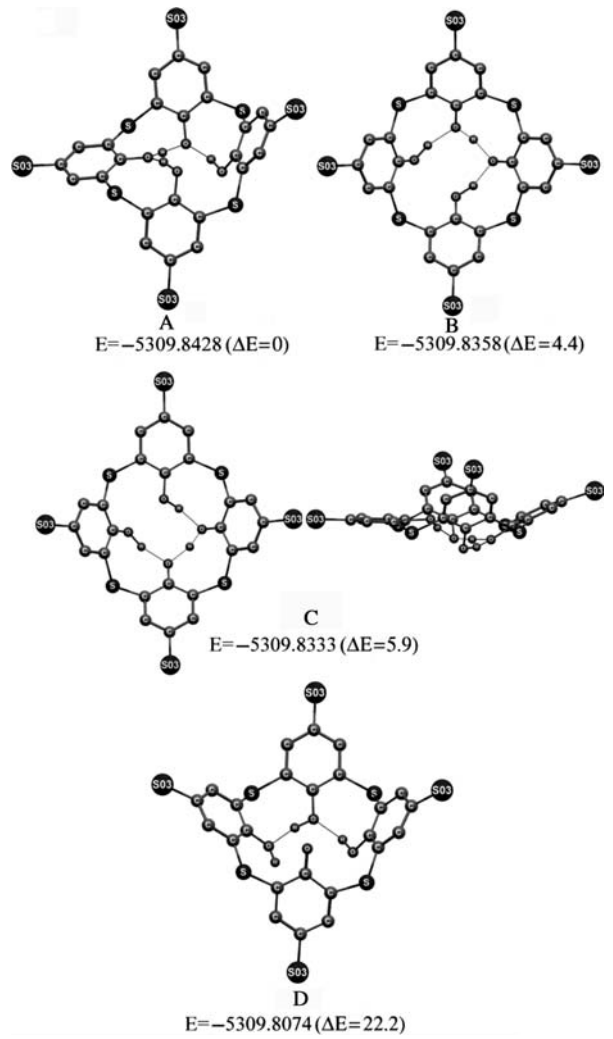

Figure 6. Optimised conformations of $TCAS^{5-}$, their electronic energies [E (a.e.u.)] and conformational energies [ΔE (kcal mol^{-1})] relative to the most stable conformer. **A**, **B**, top view; **C**, top and side view; **D**, side view. Hydrogen bonds are shown by dotted lines.

paco, *1,3-alt* and *1,2-alt*) were also found for $TCAS^{4-}$ (Table 2). The structure and the energy ordering for the conformers are practically the same as in the case of the neutral calixarenes (*27*). So, the introduction of four *p*-sulphonato groups to the thiacalix[4]arenes has not dramatically changed their conformational behaviour, except that in addition to the usual *cone* of C_4 symmetry, a much less energetically stable *cone* of C_2 symmetry was also optimised (Table 2).

In the case of $TCAS^{5-}$, strong distortions of the structure of the stable conformations, changes in their energy ordering and decrease in energy gaps between the conformers relative to $TCAS^{4-}$ are observed (Figure 6). Starting geometries of *paco*, deprotonated within the intramolecular hydrogen-bonded $(OH\cdots O)_3$ cycle, and *1,2-alt* during optimisation transform to the same conformation (**A** in Figure 6) intermediate between *paco* and *1,2-alt*. The starting *1,3-alt* after optimisation also adopts the form very close to **A** (not shown in Figure 6), with a negligible energy difference of less than 0.3 kcal mol^{-1} between the two structures. The starting *cone*-C_4 and *cone*-C_2 also become almost degenerate conformers **B** and **C** (Figure 6). All the above-mentioned conformations are much more energetically stable than *paco* conformer **D** (Figure 6). The latter is formed from the *paco* conformation of $TCAS^{4-}$ by the deprotonation of the phenolic unit, which does not participate in the $(OH\cdots O)_3$ cyclic array of hydrogen bonds. The large energy gap between **D** and all other conformations, where the deprotonated hydroxy group forms the intramolecular H-bonds with neighbouring OH moieties, demonstrates the importance of the hydrogen bonding in the stabilisation of various conformations and in protonation–deprotonation processes. It is interesting to note that the *1,3-alt* conformation, typical for calix[4]arenes and thiacalix[4]-arenes, 'disappears' in the case of $TCAS^{5-}$.

The *1,2-alt*, *paco* and *1,3-alt* conformers regain their more or less typical for the calixarene structure in the case of $TCAS^{6-}$ (**A**, **B** and **G**, respectively, in Figure 7) and $TCAS^{8-}$ (Table 3). In both the cases, the former two conformations are among the most energetically stable forms of the molecules, which agree well with the solid-state (*paco*) and solution (*1,2-alt*) structures of the complexes obtained in the present work. In contrast to $TCAS^{4-}$, the *cone* conformation of $TCAS^{6-}$ is represented by three structures (**C**, **E** and **F** in Figure 7), and none of the latter is energetically preferable. The *cone* of $TCAS^{8-}$ is not the most energetically stable conformation either, though the energy gap between this conformer and other forms of $TCAS^{8-}$ is rather small. In fact, in the absence of the intramolecular H-bonds, all conformers of the completely deprotonated TCAS are almost equally stable (Table 3). So, either the host–guest interactions or intermolecular hydrogen bonding in water–methanol solution can easily change the energy ordering of the

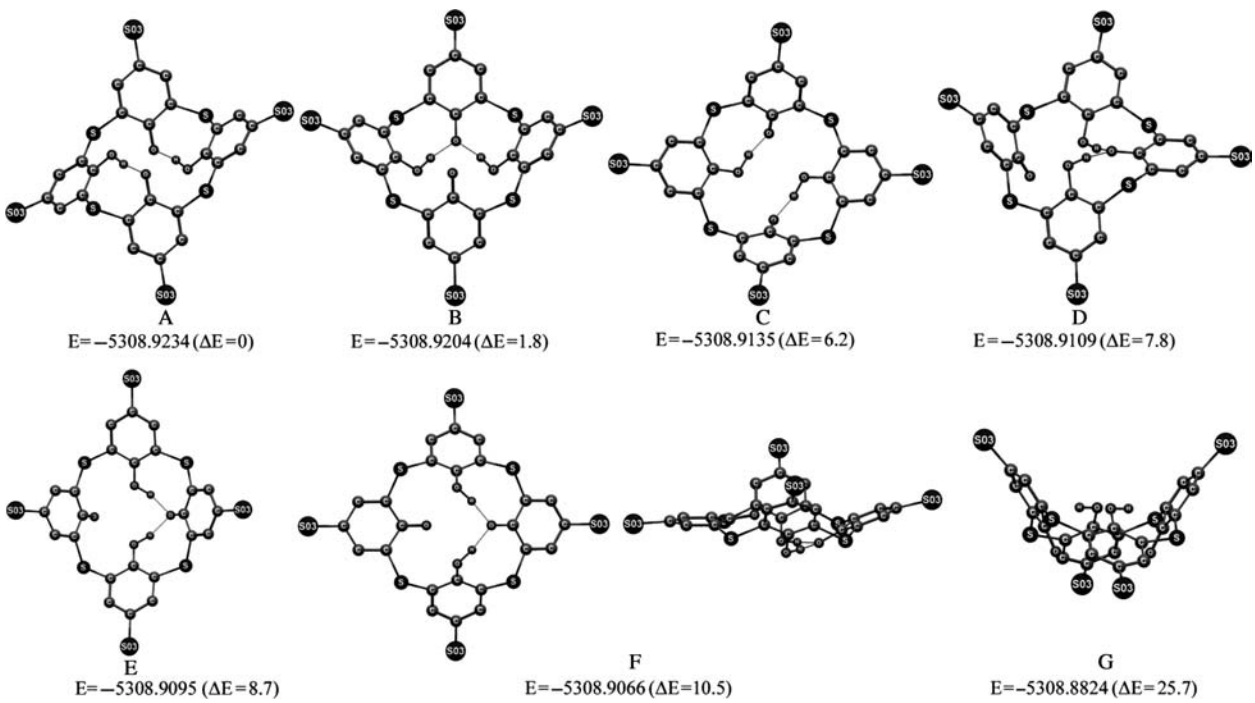

Figure 7. Optimised conformations of $TCAS^{6-}$, their electronic energies [*E* (a.e.u.)] and conformational energies [ΔE (kcal mol^{-1})] relative to the most stable conformer. **A**, **B**, **D**, **G**, side view; **C**, **E**, top view; **F**, top and side view. Hydrogen bonds are shown by dotted lines.

Table 3. Optimised conformations of $TCAS^{8-}$ and their conformational energies (ΔE) relative to the electronic energy (E) of the most stable conformer.

Conformations	E (a.e.u.)	ΔE (kcal mol^{-1})
1,3-alt	−5306.75102	0
1,2-alt	−5306.74911	1.2
Paco	−5306.74863	1.5
Cone-C_2	−5306.74422	4.3
Cone-C_4	−5306.73742	8.5

conformations (Table 3) predicted for the isolated molecule.

Conclusions

The X-ray data in the solid state and the ^{1}H NMR measurements in the solution represent the example of the guest-induced conformational shift of the host, which is not gained from the crystal packing. The X-ray analysis indicates that $TCAS^{6-}$ adopts the *partial cone* conformation in the inclusion complex with $[Zn(dipy)_3]^{2+}$, while the *pinched cone* of $TCAS^{5-}$ is predominant in its inclusion complexes with $[Co(dipy)_3]^{3+}$ and $[Ru(dipy)_3]^{2+}$. The complex $[Zn(dipy)_3]^{2+}$ is more bulky [the metal–nitrogen bond increases in the order Co(III) < Ru(II) < Zn(II)], and thus it does not fit the cavity of the *cone* of TCAS, inducing the *cone → partial cone* conformational shift. Both our experiments and DFT computations demonstrate that the conformational behaviour of TCAS molecules strongly depends on the deprotonation extent. In particular, both *partial cone* and *1,2-alternate* are among the most stable conformations of $TCAS^{6-}$. The ^{1}H NMR data in the solution reveal that the further deprotonation of phenolic groups results in *1,2-alternate*-$TCAS^{8-}$ bound with the coordinatively unsaturated $[Zn(dipy)_2]^{2+}$ or $[Zn(dipy)]^{2+}$, produced by the dissociation of $[Zn(dipy)_3]^{2+}$.

Acknowledgements

The authors are indebted to all the staff members of the Supercomputer Centre of the Kazan Scientific Centre of the Russian Academy of Sciences, and especially to Dr D. Chachkov for the technical assistance in computations. The financial support of the President of the Russian Federation for young scientists (Grant No. 5124.2008.03 for E.Z.), the RFBR (Grant No. 07-03-91560) and the Deutsche Forschungsgemeinschaft (Grant No. 3296/1-1) is gratefully acknowledged.

Supporting Information

The COSY, HMBC, HSQC spectra of the TCAS and $[Zn(dipy)_3]^{2+}$ mixture in aqueous methanol solutions are available as Supplementary Information (online).

References

(1) Mandolini, L., Ungaro, R., Eds.; *Calixarenes in Action*; Imperial College Press: London, 2000; Vicens, J., Harrowfield, J., Eds; *Calixarenes in the Nanoworld*; Springer: Dordrecht, 2007.

(2) Atwood, J.L.; Orr, G.W.; Hamada, F.; Vincent, R.L.; Bott, S.G.; Robinson, K.D. *J. Am. Chem. Soc.* **1991**, *113*, 2760–2761; Orr, G.W.; Barbour, L.J.; Atwood, J.L. *Science* **1999**, *285*, 1049–1051; Dalgarno, S.J.; Atwood, J.L.; Raston, C.L. *Cryst. Growth Des.* **2006**, *6*, 174–180; Atwood, J.L.; Barbour, L.J.; Hardie, M.J.; Raston, C.L. *Coord. Chem. Rev.* **2001**, *222*, 3–32; Dalgarno, S.J.; Atwood, J.L.; Raston, C.L. *Chem. Commun.* **2006**, 4567–4574.

(3) Nichols, P.J.; Raston, C.L.; Steed, J.W. *Chem. Commun.* **2001**, 1062–1063; Smith, C.B.; Barbour, L.J.; Makha, M.; Raston, C.L.; Sobolev, A.N. *Chem. Commun.* **2006**, 950–952.

(4) Smith, C.B.; Makha, M.; Raston, C.L.; Sobolev, A.N. *New J. Chem.* **2007**, *31*, 535–542; Makha, M.; Alias, Y.; Raston, C.L.; Sobolev, A.N. *New J. Chem.* **2007**, *31*, 662–668.

(5) Liu, Y.; Guo, D.-S.; Zhang, H.-Y.; Ding, F.; Chen, K.; Song, H.-B. *Chem. A Eur. J.* **2007**, *13*, 466–472; Liu, Y.; Guo, D.-S.; Yang, E.-C.; Zhang, H.-Y.; Zhao, Y.-L. *Eur. J. Org. Chem.* **2005**, 162–170; Lui, Y.; Wang, H.; Zhang, H.-Z.; Wang, L.-H. *Cryst. Growth Des.* **2005**, *5*, 231–235; Liu, Y.; Chen, K.; Guo, D.-S.; Song, H.-B. *Cryst. Growth Des.* **2007**, *7*, 2601–2608.

(6) Wu, M.; Yuan, D.; Han, L.; Wu, B.; Xu, Y.; Hong, M. *Eur. J. Inorg. Chem.* **2006**, (3), 526–530; Guo, Q.; Yhu, W.; Ma, S.; Yan, D.; Dong, S.; Xu, M. *J. Mol. Struct.* **2004**, *690*, 63–68; Yuan, D.; Xu, Y.; Hong, M.; Bi, W.; Zhou, Y. *Eur. J. Inorg. Chem.* **2006**, (6), 1112–1117; Yuan, D.-Q.; Wu, M.-Y.; Jiang, F.-L.; Hong, M.-C. *J. Mol. Struct.* **2008**, *877*, 132–137; Guo, Q.; Zhu, W.; Dong, S.; Ma, S.; Yan, X. *J. Mol. Struct.* **2003**, *650*, 159–164.

(7) (a) Liu, Y.; Guo, D.-S.; Zhang, H.-Y. *J. Mol. Struct.* **2005**, *734*, 241–245. (b) Lui, Y.; Guo, D.-S.; Zhang, H.-Y.; Kang, S.; Song, H.-B. *Cryst. Growth Des.* **2006**, *6*, 1399–1406.

(8) Guo, D.-S. Liu, Y. *Cryst. Growth Des.* **2007**, *7*, 1038–1041.

(9) Morohashi, N.; Narumi, F.; Iki, N.; Hattori, T.; Miyano, S. *Chem. Rev.* **2006**, *106*, 5291–5316; Lhotak, P. *Eur. J. Org. Chem.* **2004**, 1675–1692.

(10) Arena, G.; Cali, R.; Lombardo, G.G.; Rizzarelli, E.; Sciotto, D.; Ungaro, R.; Casnati, A. *Supramol. Chem.* **1992**, *1*, 19–24; Arena, G.; Casnati, A.; Mirone, L.; Sciotto, D.; Ungaro, R. *Tetrahedron Lett.* **1997**, *38*, 1999–2002.

(11) Matsumiya, H.; Terazono, Y.; Iki, N.; Miyano, S. *J. Chem. Soc. Perkin Trans. 2* **2002**, 1166–1172.

(12) Chen, X.-M.; Wang, R.-Q.; Yu, X.-L. *Acta Crystallogr. Sect. C: Cryst. Struct. Commun.* **1995**, *51*, 1545–1547.

(13) Harrowfield, J.M.; Sobolev, A.N. *Aust. J. Chem.* **1994**, *47*, 763–767.

(14) Du, M.; Zhao, X.-J.; Cai, H. *Z. Kristallogr. New Cryst. Struct.* **2004**, *219*, 463–465.

(15) (a) Mustafina, A.R.; Skripacheva, V.V.; Gubaidullin, A.T.; Latipov, Sh.K.; Toropchina, A.V.; Yanilkin, V.V.; Solovieva, S.E.; Antipin, I.S.; Konovalov, A.I. *Inorg. Chem.* **2005**, *44*, 4017–4023. (b) Mustafina, A.R.; Skripacheva, V.V.; Burilov, V.A.; Gubaydullin, A.T.; Nastapova, N.V.; Yanilkin, V.V.; Solovieva, S.E.; Antipin, I.S.; Konovalov, A.I. *Russ. Chem. Bull. Int. Ed. (Engl. Transl.)* **2008**, 1863–1870.

(16) Iki, N.; Fujimoto, T.; Miyano, S. *Chem. Lett.* **1998**, *27*, 625–626.

(17) Bray, R.G.; Ferguson, J.; Hawkins, C.J. *Aust. J. Chem.* **1969**, *22*, 2091–2103.
(18) Sheldrick, G.M. SADABS. *Program for Empirical X-ray Absorption Correction*; Bruker-Nonius: Madison, WI, 2004.
(19) Sheldrick, G.M. SHELXTL v.6.12. *Structure Determination Software Suite*; Bruker AXS: Madison, WI, 2000.
(20) Farrugia, L.J. WinGX 1.64.05. *J. Appl. Crystalogr.* **1999**, *32*, 837–838.
(21) APEX2 (Version 2.1), SAINTPlus, *Data Reduction and Correction Program (Version 7.31A), Bruker advanced X-ray solutions*; Bruker AXS, Inc.: Madison, WI, 2006.
(22) Spek, A.L. *J. Appl. Cryst.* **2003**, *36*, 7–13.
(23) GAUSSIAN 03, *Revision B.05*; Gaussian, Inc.: Wallingford, CT, 2004.
(24) Becke, A.D. *J. Chem. Phys.* **1993**, *98*, 5648–5662.
(25) Lee, C.; Yang, W.; Parr, R.G. *Phys. Rev. B* **1988**, *41*, 785–789.
(26) Liu, C.; Luo, F.; Bi, Y.; Liao, W.; Zhang, H. *J. Mol. Struct.* **2008**, *888*, 313–317.
(27) Katsyuba, S.; Kovalenko, V.; Chernova, A.; Vandyukova, E.; Zverev, V.; Shagidullin, R.; Antipin, I.; Solovieva, S.; Stoikov, I.; Konovalov, A. *Org. Biomol. Chem.* **2005**, *3*, 2558–2565.